Hyperbolic metamaterials based on quantum-dot plasmon-resonator nanocomposites

S. V. Zhukovsky,[1,*] T. Ozel,[2] E. Mutlugun,[2,3] N. Gaponik,[4] A. Eychmuller,[4] A. V. Lavrinenko,[1] H. V. Demir,[2,3] and S. V. Gaponenko[5]

[1]*DTU Fotonik – Department of Photonics Engineering, Technical University of Denmark, Ørsteds Pl. 343, DK-2800 Kongens Lyngby, Denmark*

[2] *Department of Electrical and Electronic Engineering, Department of Physics, and UNAM – Institute of Material Science and Nanotechnology, Bilkent University, Bilkent, Ankara, 06800 Turkey*

[3]*Luminous Semiconductor Lighting and Display Center of Excellence, School of Electronics Engineering, and School of Physical and Mathematical Sciences, Nanyang Technological University, Nanyang Ave., 639798 Singapore*

[4]*Physical Chemistry, Technical University of Dresden, Bergstr. 66b, 01062 Dresden, Germany*

[5]*Stepanov Institute of Physics, National Academy of Sciences of Belarus, Pr. Nezavisimosti 68, Minsk 220072, Belarus*

[*]*sezh@fotonik.dtu.dk*

Abstract: We theoretically demonstrate that nanocomposites made of colloidal semiconductor quantum dot monolayers placed between metal nanoparticle monolayers can function as multilayer hyperbolic metamaterials. Depending on the thickness of the spacer between the quantum dot and nanoparticle layers, the effective permittivity tensor of the nanocomposite is shown to become indefinite, resulting in increased photonic density of states and strong enhancement of quantum dot luminescence. This explains the results of recent experiments [T. Ozel et al., ACS Nano **5**, 1328 (2011)] and confirms that hyperbolic metamaterials are capable of increasing the radiative decay rate of emission centers inside them. The proposed theoretical framework can also be used to design quantum-dot/nanoplasmonic composites with optimized luminescence enhancement.

OCIS codes: (160.3918) Metamaterials; (160.4236) Nanomaterials; (160.1190) Anisotropic optical materials; (250.5590) Quantum-well, -wire and -dot devices.

References and links

1. D. R. Smith, D. Schurig, J. J. Mock, P. Kolinko, and P. Rye, "Partial focusing of radiation by a slab of indefinite media," Appl. Phys. Lett. **84**(13), 2244–2246 (2004).
2. M. A. Noginov, H. Li, Yu. A. Barnakov, D. Dryden, G. Nataraj, G. Zhu, C. E. Bonner, M. Mayy, Z. Jacob, and E. E. Narimanov, "Controlling spontaneous emission with metamaterials," Opt. Lett. **35**(11), 1863–1865 (2010).
3. Z. Jacob, J.-Y. Kim, G.V. Naik, A. Boltasseva, E.E. Narimanov, and V.M. Shalaev, "Engineering the photonic density of states with metamaterials," Appl. Phys. B **100**(1), 215–218 (2010).
4. Z. Jacob, I. I. Smolyaninov, and E.E. Narimanov, "Broadband Purcell effect: Radiative decay engineering with metamaterials," Appl. Phys. Lett. **100**(18), 181105 (2012).
5. C. Simovski, S. Maslovski, I. Nefedov, and S. Tretyakov, "Optimization of radiative heat transfer in hyperbolic metamaterials for thermophotovoltaic applications," Opt. Express **21**(12), 14988–15013 (2013).
6. Y. Guo and Z. Jacob, "Thermal hyperbolic metamaterials," Opt. Express **21**(12), 15014–15019 (2013).

#208695 - $15.00 USD Received 21 Mar 2014; revised 27 May 2014; accepted 6 Jul 2014; published 22 Jul 2014

7. T. Morgado, S. I. Maslovski, and M. G. Silveirinha, "Ultrahigh Casimir interaction torque in nanowire systems," Opt. Express **21**(12), 14943–14955 (2013).
8. G. D'Aguanno, N. Mattiucci, M. Bloemer, and A. Desyatnikov, "Optical vortices during a superresolution process in a metamaterial," Phys. Rev. A **77**(4), 043825 (2008).
9. N. Mattiucci, G. D'Aguanno, M. Scalora, M. J. Bloemer, and C. Sibilia, "Transmission function properties for multi-layered structures: Application to super-resolution," Opt. Express **17**(20), 17517–17529 (2009).
10. S. Ramakrishna, J. Pendry, M. Wiltshire, and W. Stewart, "Imaging the near field," J. Mod. Opt. **50**(9), 1419–1430 (2003).
11. Z. Jacob, L. V. Alekseyev, and E. Narimanov, "Optical Hyperlens: Far-field imaging beyond the diffraction limit," Opt. Express **14**(18), 8247–8256 (2006).
12. N. Mattiucci, M. J. Bloemer, N. Aközbek, and G. D'Aguanno, "Impedance matched thin metamaterials make metals absorbing," Sci. Rep. **3**, 3203 (2013).
13. E. E. Narimanov, H. Li, Y. A. Barnakov, T. U. Tumkur, and M. A. Noginov, "Reduced reflection from roughened hyperbolic metamaterial," Opt. Express **21**(12), 14956–14961 (2013).
14. I. I. Smolyaninov and E. E. Narimanov, "Metric signature transitions in optical metamaterials," Phys. Rev. Lett. **105**(6), 067402 (2010).
15. I. I. Smolyaninov and Yu-Ju Hung, "Modeling of time with metamaterials," J. Opt. Soc. Am. B **28**(7), 1591–1595 (2011).
16. C. L. Cortes, W. Newman, S. Molesky, and Z. Jacob, "Quantum nanophotonics using hyperbolic metamaterials," J. Opt. **14**(6), 063001 (2012).
17. V. Drachev, V. A. Podolskiy, and A. V. Kildishev, "Hyperbolic Metamaterials: new physics behind a classical problem," Opt. Express **21**(12), 15048–15064 (2013).
18. M. A. Noginov, Yu. A. Barnakov, G. Zhu, T. Tumkur, H. Li, and E. E. Narimanov, "Bulk photonic metamaterial with hyperbolic dispersion," Appl. Phys. Lett. **94**(15), 151105 (2009).
19. O. Kidwai, S. V. Zhukovsky, and J. E. Sipe, "Dipole radiation near hyperbolic metamaterials: applicability of effective-medium approximation," Opt. Lett. **36**(13), 2530–2532 (2011).
20. A. N. Poddubny, P. A. Belov, and Yu. S. Kivshar, "Spontaneous radiation of a finite-size dipole emitter in hyperbolic media," Phys. Rev. A **84**(2), 023807 (2011).
21. I. Iorsh, A. Poddubny, A. Orlov, P. Belov, and Yu. Kivshar, "Spontaneous emission enhancement in metal-dielectric metamaterials," Phys. Lett. A **376**(3), 185–187 (2012).
22. O. Kidwai, S. V. Zhukovsky, and J. E. Sipe, "Effective-medium approach to planar multilayer hyperbolic metamaterials: Strengths and limitations," Phys. Rev. A **85**(5), 053842 (2012).
23. D. V. Guzatov, S. V. Vaschenko, V. V. Stankevich, A. Y. Lunevich, Y. F. Glukhov, and S. V. Gaponenko, "Plasmonic enhancement of molecular fluorescence near silver nanoparticles: theory, modeling, and experiment," J. Phys. Chem. C **116**(19), 10723–10733 (2012).
24. J. Kim, V. P. Drachev, Z. Jacob, G. V. Naik, A. Boltasseva, E. E. Narimanov, and V. M. Shalaev, "Improving the radiative decay rate for dye molecules with hyperbolic metamaterials," Opt. Express **20**(7), 8100–8116 (2012).
25. S. Zhukovsky, O. Kidwai, and J. E. Sipe, "Physical nature of volume plasmon polaritons in hyperbolic metamaterials," Opt. Express **21**(12), 14982–14987 (2013).
26. O. Kulakovich, N. Strekal, A. Yaroshevich, S. Maskevich, S. Gaponenko, I. Nabiev, U. Woggon, and M. Artemyev, "Enhanced luminescence of CdSe quantum dots on gold colloids," Nano Lett. **2**(12), 1449–1452 (2002).
27. M. Lunz, V. A. Gerard, Y. K. Gunko, V. Lesnyak, N. Gaponik, A. S. Susha, A. L. Rogach, and A. L. Bradley, "Surface plasmon enhanced energy transfer between donor and acceptor CdTe nanocrystal quantum dot monolayers," Nano Lett. **11**(8), 3341–3345 (2011).
28. T .Ozel, P. L. Hernandez Martinez, E. Mutlugun, O. Akin, S. Nizamoglu, I. O. Ozel, and H. V. Demir, "Observation of selective plasmon-exciton coupling in nonradiative energy transfer: Donor-selective vs. acceptor-selective plexcitons," Nano Lett. **13**(6), 3065–3071 (2013).
29. M. L. Brongersma, J. W. Hartman, and H. A. Atwater, "Electromagnetic energy transfer and switching in nanoparticle chain arrays below the diffraction limit," Phys. Rev. B **62**(24), R16356–R16359 (2000).
30. M. Navarro-Cìa, M. Beruete, S. Agrafiotis, F. Falcone, M. Sorolla, and S. A. Maier, "Broadband spoof plasmons and subwavelength electromagnetic energy confinement on ultrathin metafilms," Opt. Express **17**(20), 18184–18195 (2009).
31. T. Ozel, S. Nizamoglu, M. A. Sefunc, O. Samarskaya, I. O. Ozel, E. Mutlugun, V. Lesnyak, N. Gaponik, A. Eychmuller, S. V. Gaponenko, and H. V. Demir, "Anisotropic emission from multilayered plasmon resonator nanocomposites of isotropic semiconductor quantum dots," ACS Nano **5**(2), 1328–1334 (2011).
32. K. Dolgaleva and R. W. Boyd, "Local-field effects in nanostructured photonic materials," Adv. Opt. Photon. **4**(1), 1–77 (2012).
33. J. H. Kim, J. H. Hwang, and T. Y. Lim, "A layer-by-layer self-assembly method for organic-inorganic hybrid multilayer thin films," J. Ceram. Process. Res. **10**(6), 770–773 (2009).
34. M. Fujita, S. Takahashi, Y. Tanaka, T. Asano, and S. Noda. "Simultaneous inhibition and redistribution of spontaneous light emission in photonic crystals," Science **308**(5726), 1296–1298 (2005).
35. A. F. Koenderink, M. Kafesaki, C. M. Soukolis, and V. Sandoghdar, "Spontaneous emission in the near field of

#208695 - $15.00 USD Received 21 Mar 2014; revised 27 May 2014; accepted 6 Jul 2014; published 22 Jul 2014

two-dimensional photonic crystals," Opt. Lett. **30**(23), 3210–3212 (2005).
36. S. V. Gaponenko, *Introduction to Nanophotonics* (Cambridge University Press, 2010).

1. Introduction

Hyperbolic metamaterials (HMMs) have attracted an intense scientific interest during the recent years for several reasons. First and foremost, the material properties of such metamaterials, namely, an indefinite form of their effective permittivity tensor (such that, e.g., $\varepsilon_x = \varepsilon_y < 0$ and $\varepsilon_z > 0$ [1]) give rise to an unusual hyperbolic dispersion relation, $\omega^2/c^2 = (k_x^2 + k_y^2)/\varepsilon_z + k_z^2/\varepsilon_{x,y}$ [Fig. 1(a)]. Such a dispersion relation is associated with an anomalous increase of the photonic density of states (PDOS), strongly affecting many physical phenomena that rely on it: spontaneous emission [2–4], blackbody radiation [5, 6], and Casimir forces [7]. More practical applications of HMMs include superresolution [8, 9], far-field subwavelength imaging or "hyperlensing" [10, 11], and high broadband absorbance [12] impervious to the detrimental effects of surface roughness [13]. Still other intriguing applications rely on similarities between optical dispersion relations and cosmological equations to use HMMs for tabletop optical simulation of space-time phenomena [14, 15]. New aspects of HMM research are being uncovered (see [16, 17] and references therein).

The other important reason of the interest in HMMs is that unlike many other types of metamaterials, HMMs do not require resonant "building blocks" and can therefore be practically realized using rather simple geometries. Metal-dielectric composites as simple as subwavelength multilayers [3, 4] and nanorod arrays [2, 18] have been shown to possess salient properties of HMMs in a broad frequency range. In a series of recent experiments, it was shown that placing such metal-dielectric HMMs close to luminescent centers enhance their decay rate more strongly than what is achievable using metal or dielectric alone [2, 3]. However, even though these experimental results were well explained by the theory of dipole radiation in an HMM environment [19–22], it has proven rather difficult to distinguish whether the emission rate increase can be attributed to the increase of the *radiative* decay rate (i.e., the Purcell effect) or just quenching of luminescence (as happens with an emitter near a metallic surface, see [23]). Only in the recent work by Kim et al. [24] direct evidence of the radiative rate increase was reported.

Despite the fact that the underlying geometry of an HMM can be as simple as a metal-dielectric multilayer [Fig. 1(b)], it has proven quite challenging to fabricate an HMM with reliable characteristics. The reason is that the thicknesses of the layers involved must be subwavelength not only with respect to the vacuum wavelength of the incident light, but also with respect to large-wavevector bulk plasmonic waves that exist inside HMMs and substantiate the anomalously large PDOS in them [25]. Continuous metal films of such small thickness (on the order of a few nanometers) are difficult to fabricate using state of the art growing facilities. Depositing luminescent centers on the surface of a HMM can also be challenging and may additionally be affected by plasmonic effects in the outermost HMM layer [22].

Here, we would like to point out another and perhaps an easier possibility to obtain a characterizable structure with HMM properties. It has been known for quite a while that layer-by-layer assembly of plasmonic nanoparticle (NP) monolayers can be realized by separating the monolayers by polyelectrolyte (PDDA) layers [26–28]. In a densely packed monolayer of such NPs, localized plasmon resonances in each nanoparticle would couple to support "spoof" surface plasmonic waves [29, 30], so the monolayer may be regarded as a corrugated metallic layer. Using a similar technology, semiconductor nanocrystals (NCs), which are luminescent quantum dots, can be likewise assembled into monolayers, able to function as both dielectric and emitting layers. Alternating NP and NC monolayers is thus likely to result in HMM behavior.

Indeed, a recent experimental paper by T. Ozel et al. [31] reported that the luminescence from NCs was increased by a factor of 4 when placed into such a multilayer arrangement.

#208695 - $15.00 USD Received 21 Mar 2014; revised 27 May 2014; accepted 6 Jul 2014; published 22 Jul 2014

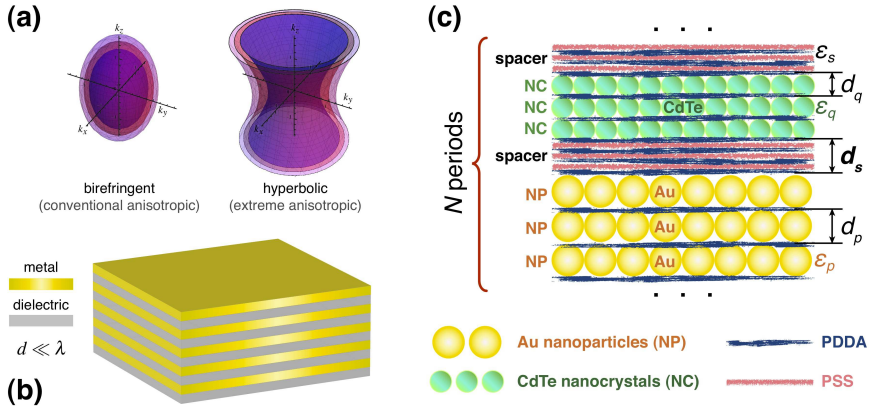

Fig. 1. (a) Isofrequency surfaces in the dispersion relation $(k_x^2+k_y^2)/\varepsilon_z+k_z^2/\varepsilon_{x,y}=\omega^2/c^2$ for conventional anisotropic medium ($\varepsilon_{x,y,z}>0$) and indefinite medium ($\varepsilon_{x,y}<0$ and $\varepsilon_z>0$). (b) Schematics of a multilayer metal-dielectric HMM. (c) Schematics of NP-spacer-NC from [31], showing the geometrical notation used in the paper.

Interestingly, the enhancement was only seen when the NC and NP layers were separated by thin dielectric spacer layers [Fig. 1(c)]. Even though an explanation based on the increased plasmon-exciton coupling between NCs and NPs was given and confirmed by time-domain numerical simulations, the role of the dielectric spacer layers was not very well understood.

In this paper, we revisit these previous experimental results and show that the measured enhancement of NC emission rate can be attributed to the multilayer structure exhibiting metallic properties without the spacer layers and HMM properties when such layers are added.It is confirmed that significant enhancement and a pronounced anisotropic character of the radiative decay of emitting NCs when adding the spacer layer can be related to the indefinite character of the effective permittivity tensor characteristic for HMMs. Dependencies of the radiative rate enhancement due to the presence of the spacer layer on its thickness, as well as other geometrical parameters of the structure, are calculated. It is also shown that making the NP-containing layers thinner, for example by reducing the number of NP monolayers, will likely result in the enhancement of all HMM-related properties of the nanocomposite, including the photoluminescence enhancement.

The paper is organized as follows. In Section 2, we briefly review the theoretical background on multilayer HMMs and calculate the effective permittivity tensor of the NC-spacer-NP multilayer composites. Section 3 follows with the estimation of the emission rate of a finite-sized emitter in a multilayer HMM, and the associated luminescence enhancement. Comparison against previous experimental results [31] is made, and guidelines towards optimizing the emission enhancement are given. Finally, in Section 4 we summarize the paper.

2. Nanocrystal/nanoparticle composites as multilayer hyperbolic metamaterials

We begin by considering an infinitely periodic system shown in Fig. 1(c) where a number (m_p) of monolayers of gold NPs with diameter $d_p=15$ nm alternate with a number (m_q) of monolayers of semiconductor (CdTe) NC quantum dots with diameter $d_q=5.5$ nm, separated by dielectric spacers with varied thickness d_s. The dielectric constants of gold, CdTe, and the spacer material are denoted by ε_p, ε_q, and ε_s, respectively.

We will follow the standard multilayer homogenization procedure [32] where the effective permittivity components of a subwavelength multilayer are determined by the relations

#208695 - $15.00 USD Received 21 Mar 2014; revised 27 May 2014; accepted 6 Jul 2014; published 22 Jul 2014

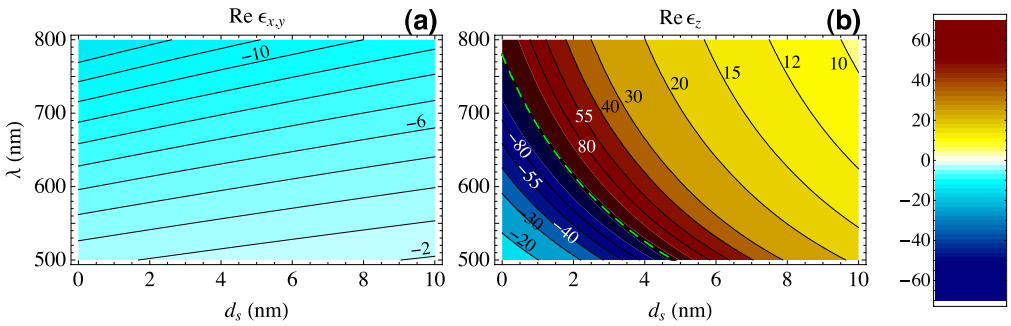

Fig. 2. Plots of the real part of (a) $\varepsilon_x = \varepsilon_y$ and (b) ε_z depending on the spacer thickness d_s and the incident light wavelength λ for the structure shown in Fig. 1(c). The green dashed line in (b) shows the singularity where $\mathrm{Re}\,\varepsilon_z^{-1} = 0$.

$$\varepsilon_x = \varepsilon_y = \frac{2d_s\varepsilon_s + m_p d_p \bar{\varepsilon}_p + m_q d_q \bar{\varepsilon}_q}{2d_s + m_p d_p + m_q d_q}, \quad \varepsilon_z^{-1} = \frac{2d_s\varepsilon_s^{-1} + m_p d_p \bar{\varepsilon}_p^{-1} + m_q d_q \bar{\varepsilon}_q^{-1}}{2d_s + m_p d_p + m_q d_q}. \tag{1}$$

The averaged permittivity $\bar{\varepsilon}_q$ of a dielectric NC monolayer can be estimated from the Bruggeman formula (see [32]):

$$f_q \frac{\varepsilon_q - \bar{\varepsilon}_q}{\varepsilon_q + 2\bar{\varepsilon}_q} + (1 - f_q)\frac{1 - \bar{\varepsilon}_q}{1 + 2\bar{\varepsilon}_q} = 0 \tag{2}$$

The plasmonic NP monolayer can be assumed to be above the percolation threshold to have conductive coupling between the NPs, so that the entire monolayer can be treated using the Drude model with the diluted metal assumption, with the resulting averaged permittivity

$$\bar{\varepsilon}_p = 1 - \frac{f_p \omega_p^2}{\omega^2 - i\gamma\omega} \tag{3}$$

where ω_p and γ are the standard Drude plasma and collision frequency for the metal. The factors $f_{p,q}$ are volume filling fractions of the particle material (metal for NPs and semiconductor for NCs) within each monolayer; for the triangular lattice, $f_{q,p} = \pi^2/(8\sqrt{3})$. Finally, the permittivity of the PDDA/PSS spacer layers is $\varepsilon_s = 2.4$ [33].

For $m_p = m_q = 3$ and the materials used in [31], the resulting permittivity tensor components are shown in Fig. 2. It can be seen at once that the parallel component $\varepsilon_{x,y}$ varies slowly and remains negative, whereas the real part of the perpendicular component ε_z changes sign at $\mathrm{Re}\,\varepsilon_z^{-1} = 0$, which happens at d_s between 1 and 5 nm, depending on the wavelength.

Therefore, the functionality of the entire material crucially depends on the spacer. Without it ($d_s = 0$), the material is effectively a strongly anisotropic metal with $|\varepsilon_z| \gg |\varepsilon_{x,y}|$ and $\varepsilon_z < \varepsilon_{x,y} < 0$. As any metal, such a material would quench the luminescence from the NCs compared to the case when NPs are absent. Conversely, adding the spacer results in $|\varepsilon_z| \gg |\varepsilon_{x,y}|$ but $\varepsilon_{x,y} < 0 < \varepsilon_z$, and the material becomes an HMM. Thus, a significant increase of the decay rate of the NCs (including the increase of radiative decay) would be expected.

We note that we have regarded a passive metal-dielectric structure with dipole emitters embedded in it, whereas in [31] the structure is active, with quantum dots used both as a constituent portion of HMM and as an ensemble of luminescent probes. A similar approach has been applied to examine radiative decay of emitters in a photonic crystal [34]. The latter was examined in more detail than the emergent notion of HMM. Notably, when a probe position was scanned from the depth of the structure to its surface or even slightly (10 nm) above, the enhancement

#208695 - $15.00 USD Received 21 Mar 2014; revised 27 May 2014; accepted 6 Jul 2014; published 22 Jul 2014

effect of a photonic crystal density of states on radiative lifetime was shown to persist steadily with smooth position dependence [35]. Given that multilayer HMMs act as photonic crystals for large-wavevector metamaterial modes [25], we expect that the considered homogenization is an adequate representation of the structure in [31] for the purpose of establishing the plausibility of the hypothesis regarding the HMM properties of the structures under consideration.

3. Enhancement of emission from nanocrystals

Having established that adding the spacer layer corresponds to the metal/HMM transition in the considered structures, we can estimate the related enhancement of spontaneous emission rate. Using the two-level model as a reasonable starting approximation for the QD response, believed to be sufficient to reveal the principal effects in the multilayer system under consideration like it is done in many previous cases (see, e.g., Chapter 5 in [36]), the QD emission rate can be approximated by the Purcell factor of a dipole emitter in close vicinity of an HMM [22]:

$$b = 1 + \frac{3}{2\sqrt{\varepsilon_c}} \mathrm{Re}\left(\int_0^\infty \frac{\tilde{\kappa} d \tilde{\kappa}}{\sqrt{\varepsilon_c - \tilde{\kappa}^2}} \left[f_\perp^2 \frac{\tilde{\kappa}^2}{\varepsilon_c} R^p + \frac{f_\parallel^2}{2} \left(R^s - \frac{\varepsilon_c - \tilde{\kappa}^2}{\varepsilon_c} R^p \right) \right] e^{-\tilde{\kappa}^2 d_q^2} \right), \qquad (4)$$

where ε_c is the ambient refractive index, $\tilde{\kappa} = \kappa c/\omega$, $f_\parallel = \cos\theta$ and $f_\perp = \sin\theta$ describe the orientation of the emitting dipole, and $R^{s,p}$ are the Fresnel reflection coefficients of the structure for the two polarizations [22]. The cut-off exponential $e^{-\tilde{\kappa}^2 d_q^2}$ stems from the finite size of NCs d_q [20] and replaces the "distance between HMM and dipole" cut-off discussed in [22].

The Fresnel coefficients can be calculated using the transfer matrix method for multilayer structures with both finite [20, 21] and infinite [22] number of periods. The salient properties of HMMs stem from the existence of high-κ band where HMM supports propagating waves and $\mathrm{Im}\, R^p$ is significantly non-zero [25]. In a homogeneous HMM, it would span from $\kappa_c = (\omega/c)\sqrt{\varepsilon_z}$ all the way to infinity. In multilayers with finite layer thickness, however, the high-κ band will be limited by the thickest layer, in our case $3d_p$ [3, 19, 22].

Indeed, Figs. 3(a) and 3(b) show the existence of such a band for $d_s = 8$ nm in stark contrast with its absence for $d_s = 0$. Comparing the reflection properties of the structures with finite number of periods N [Fig. 3(c)], we see that the overall character of the band is preserved for finite N, and the spectrum for $N = 5$ qualitatively coincides with that for $N = \infty$.

To be able to compare the spontaneous emission enhancement of Eq. (4) with the luminescence enhancement in [31], one needs to distinguish between the radiative (enhancement) and non-radiative (quenching) Purcell factor. To do so, we have artificially negated all losses in the system; the resulting enhancement thus has to be purely radiative. Even though the action of an HMM on an emitter is very likely to result in coupling to large-wavevector modes that do not couple outside of the structure in the ideal case, making the luminescence enhancement hard to observe, the associated emission enhancement is still radiative from the physical point of view because modes in the metamaterial are external with respect to the emitter. Indeed, luminescence enhancement was reported to accompany the lifetime shortening of emitters placed close to multilayer HMMs [24]. Hence, the rate between $b(d_s \neq 0)$ and $b(d_s = 0)$ can be regared as an estimate of the luminescence enhancement factor due to the HMM character of the infinite-period NP-spacer-NC nanocomposite. Shown in Fig. 4 for two different orientations of the emitting dipole, it is seen that the enhancement grows as d_s becomes larger, and then falls back towards unity as spacer layers become so thick that the high-κ band is suppressed. It can be seen that for $d_s < 10$ nm, the enhancement is markedly stronger at shorter wavelength for one of the orientation of the emitting dipoles, explaining a slight blue shift of the luminescence peak in experiments [31]. It can also be seen that the enhancement is different for the

#208695 - $15.00 USD Received 21 Mar 2014; revised 27 May 2014; accepted 6 Jul 2014; published 22 Jul 2014

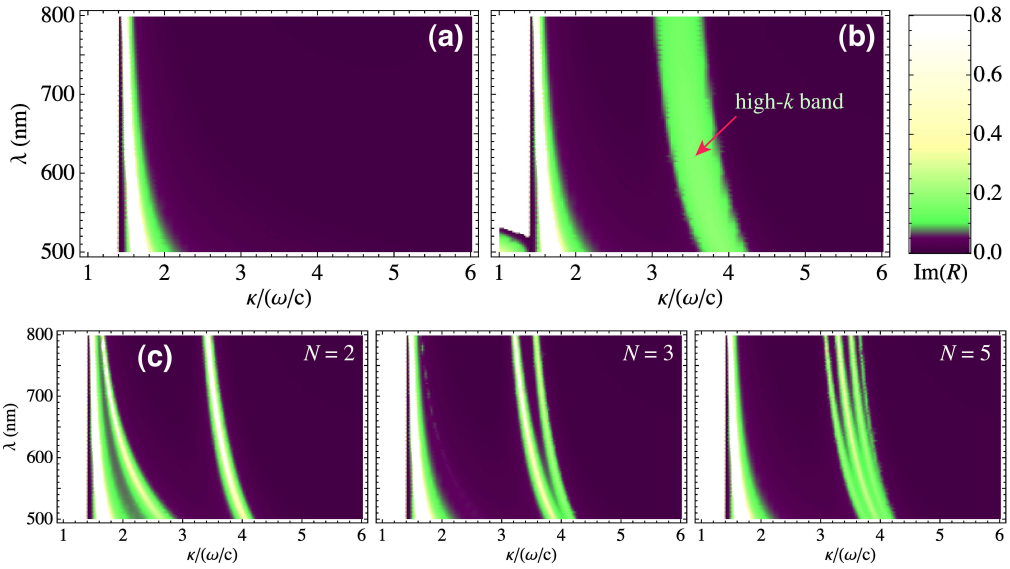

Fig. 3. High-κ wave vector dependencies of $\mathrm{Im}\,R^p$ for (a) $d_s = 0$, $N = \infty$; (b) $d_s = 8$ nm, $N = \infty$; (c) $d_s = 8$ nm and $N = 2, 3, 5$.

different orientation of the emitter, confirming the observed anisotropy in photoluminescence spectra [31].

The calculated values of the enhancement factor are between 1.5 and 2.0 (Fig. 4). For comparison with the theoretical modeling we recall the results of experimental studies of luminescence lifetime parameters for the multilayer structure and for its individual components. The lifetime for a sole quantum dot layer was measured to be 7.66 ± 0.24 ns. The lifetime of a single period of the structure, i.e. a quantum dot layer over a metal Au nanoparticles layer separated by a dielectric spacer was measured to be 5.31 ± 0.17 ns. The 5-period structure was found to feature 2.85 ± 0.11 ns [31]. Therefore one can see that the typical plasmonic enhancement of decay rate known for single-layered metal-dielectric (semiconductor) structures (see, e.g. [23, 36]) cannot be responsible for the lifetime modification observed for the 5-period structure. For the reasonable comparison with the modeling, experimental results for lifetime in the periodic structure should be compared with the reference data for a single dot-spacer-metal period rather than with intrinsic lifetime of sole quantum dot layer. Comparing 2.85 versus 5.31 ns one arrives at 1.86-fold reduction in the lifetime and, accordingly 1.86-fold enhancement of the decay rate. This falls into the theoretically predicted values of decay rate enhancement, $\beta = 1.5 \ldots 2$, presented in Fig. 4.

One should also keep in mind that in all metal-dielectric structures, the radiative decay can be severely surpassed by enhanced non-radiative decay, thus resulting in luminescence quenching (rather than enhancement) in addition to lifetime shortening. To avoid such quenching, a luminescent probe should be separated from a metal body by about 5–6 nm as has been found and suggested in our previous works [23, 26]. In the structure under analysis, where QDs are separated by 5-layer polyelectrolyte spacers, we are therefore sure that non-radiative processes do not dominate. Therefore the observed enhancement in decay rate cannot be attributed to metal-induced quenching but would mainly result from the HMM effects.

Therefore, we can conclude that the observed 1.86-fold increase in the decay rate reasonably agrees with the theoretical modeling and cannot be attributed entirely to the plasmonic effect in a single layer; rather, it is the result of the fact that the multilayer structure acquires the

#208695 - $15.00 USD Received 21 Mar 2014; revised 27 May 2014; accepted 6 Jul 2014; published 22 Jul 2014

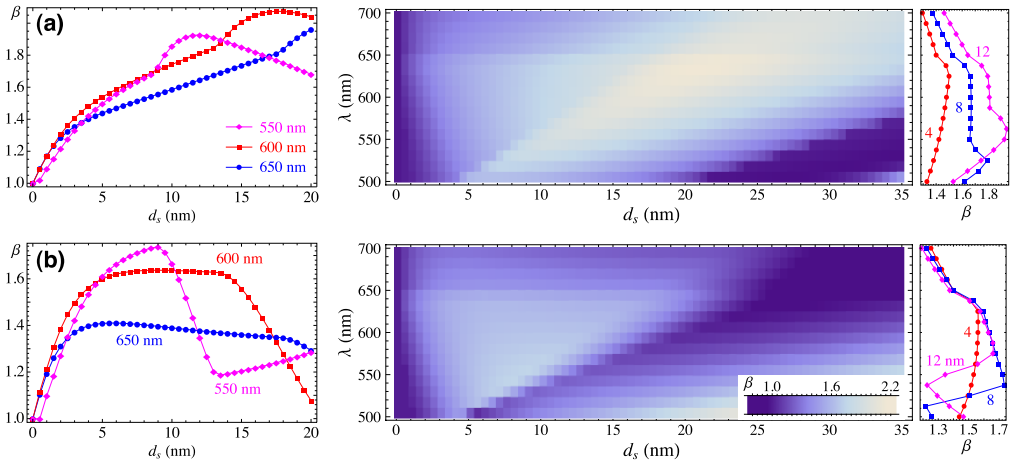

Fig. 4. Ratio of decay rate for the structure with and without spacer [$\beta = b(d_s)/b(d_s = 0)$] in absence of material losses and therefore corresponding to the radiative rate enhancement for (a) parallel ($f_{\parallel} = 1, f_{\perp} = 0$) and (b) perpendicular ($f_{\perp} = 1, f_{\parallel} = 0$) orientation of the emitting dipole. The middle column shows the 2D dependence $\beta(d_s, \lambda)$; the left column shows $\beta(d_s)$ at three wavelengths; the right column shows $\beta(\lambda)$ for three values of d_s.

properties of a hyperbolic medium. This conclusion is additionally supported by the growing anisotropy of emission in terms of more strongly polarized emission for a larger number of layers. This observation means again that the multilayer structure does gain additional features which do not reduce to simple sum of the properties inherent in a single period. We bear in mind the this semi-qualitative analysis is by no means exhaustive, and further experiments shall be performed to examine the complicated spatially-angular features of output luminescence owing to specific HMM modes. These experiments are planned with thicker structures since the approximately 400 nm thickness of the structure examined may not demonstrate HMM mode properties to their full extent.

On the other hand, we expect that an even greater agreement with the experimental results can be obtained by using a more refined model, which would take into account the positions of individual NCs within the structure [21] by generalizing it to account for finite-N structures. Another potential source of disagreements is the spoof character of SPPs in a highly corrugated NP monolayer compared to a smooth layer, potentially leading to a stronger field confinement and a more pronounced PDOS increase as a result. We believe that these two approximations are the strongest simplifications involved in the present model, and going beyond them is an interesting topic for further studies.

It also becomes clear that the HMM character of the structure, and hence the predicted photoluminescence enhancement, becomes stronger if the high-κ band (see Fig. 3) is more pronounced. Hence, we can use the presented theoretical findings to further optimize the composite design using this criterion. As mentioned above, we know that the high-κ band is wider for structures with thinner layers, so it can be expected that lowering m_p from 3 to 1 would improve the response of the structure. It can also be seen that lower $|\varepsilon_z|$ brings the high-κ band towards the smaller κ, making it less susceptible to the NC size cut-off in Eq. (4).

Figure 5 shows that indeed, lowering m_q from 3 to 1 significantly increases both the width of the high-κ band and the magnitude of ImR inside it [cf. Figs. 3(b), 5(a), and 5(d)]. As established above, this can drastically boost the spontaneous emission and NC luminescence enhancement. On the contrary, lowering m_q [cf. Figs. 5(a)–5(c)] does not influence the HMM

#208695 - $15.00 USD Received 21 Mar 2014; revised 27 May 2014; accepted 6 Jul 2014; published 22 Jul 2014

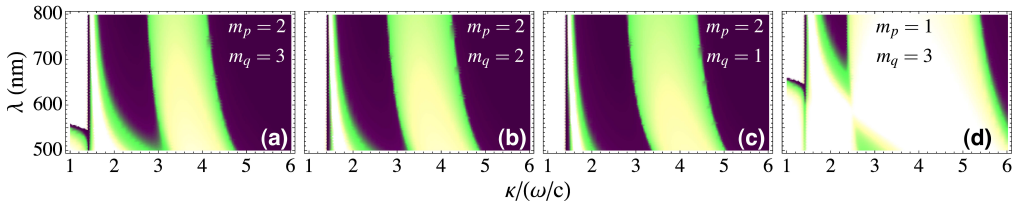

Fig. 5. Same as Fig. 3(b) but for different number of NP and NC monolayers m_p and m_q.

band much, although it does make it more pronounced at the higher-wavelength edge. This is because of the overall decrease of losses in the material due to the reduction of the overall content of CdTe. One can note, however, that many HMM characteristics were shown to be robust against the presence of ohmic losses in the metal [9, 22].

4. Conclusions

We have demonstrated that nanocomposites consisting of layers of self-assembled colloidal semiconductor quantum dots arranged between layers of likewise assembled metal nanoparticles [Fig. 1(c)] can function as multilayer HMMs. Depending on the geometric parameters of the composite, such as the number of quantum dot and nanoparticle layers, as well as the thickness of the spacer layer between quantum dots and nanoparticles, the effective permittivity tensor of the entire nanocomposite may become indefinite (see Fig. 2). This leads to an increase in the photonic density of states, in turn resulting in strong enhancement and pronounced polarization anisotropy of quantum dot luminescence [24]. This offers an alternative explanation of the results of recent experiments [31]. At the same time, these results allow to see these experiments in new light, directly confirming that HMMs are capable of increasing the radiative decay rate of emission centers placed inside them, in the same way as the more recent demonstration by Kim et al in [24].

The proposed theoretical framework, looking at NP-spacer-NC nanocomposites from the point of view of HMMs, allows easy design of such composites with predetermined properties. For example, lowering the number of NP monolayers (m_p) is shown to significantly enhance all HMM-related properties by broadening and srengthening the large-wavevector band responsible for HMM properties. On the other hand, varying the number of NC layers (m_q) does not influence the HMM properties much, but can be used to vary the overall number of emitting centers inside the nanocomposite.

Acknowledgments

The authors thank F. J. Arregui for helpful suggestions. This work has been partially supported by the Basic Research Foundation of Belarus. S.V. Z. wishes to acknowledge financial support from the People Programme (Marie Curie Actions) of the European Union's 7th Framework (EU FP7) Programme FP7-PEOPLE-2011-IIF under REA grant agreement No. 302009 (Project HyPHONE). N.G., A.E., and H.V. D acknowledge partial financial support from EU FP7 Network of Excellence "Nanophotonics for Energy Efficiency (N4E)". H.V.D., E.M., and T.O. gratefully acknowledge Singapore National Research Foundation (NRF) under programs NRF-RF-2009-09 and NRF-CRP-6-2010-02, as well as TBA – Turkish Academy of Sciences